Eur. Phys. J. D **7**, 361–367 (1999)

THE EUROPEAN PHYSICAL JOURNAL D

EDP Sciences

Microfabricated magnetic waveguides for neutral atoms

J.H. Thywissen[a], M. Olshanii, G. Zabow, M. Drndić, K.S. Johnson[b], R.M. Westervelt, and M. Prentiss

Department of Physics, Harvard University, Cambridge, MA 02138, USA

Received 1st December 1998 and Received in final form 23 February 1999

Abstract. We describe how tightly confining magnetic waveguides for atoms can be created with microfabricated or nanofabricated wires. Rubidium atoms guided in the devices we have fabricated would have a transverse mode energy spacing of 50 μK. We discuss the creation of a single-mode waveguide for atom interferometry whose depth is comparable to magneto-optical trap (MOT) temperatures. We also discuss the application of microfabricated waveguides to low-dimensional systems of quantum degenerate gases, and show that confinement can be strong enough to observe fermionization in a strongly interacting bosonic ensemble.

PACS. 03.75.Be Atom and neutron optics – 32.80.Pj Optical cooling of atoms; trapping

1 Introduction

Recently, there has been much interest in the physics of neutral atoms tightly confined in one or more dimensions [1–4]. Simultaneously, there has been continued interest in waveguides for atoms [5–14]. In this work, we propose a tightly confining magnetic waveguide whose transverse energy level spacing is comparable to the temperature of a magneto-optical trap.

Atoms have been guided through the hollow core of optical fibers [5–7], where quasi-resonant laser light repels the atoms from the walls. Cores as small as 1 μm have been used [15]; however, the minimum length scale of confinement, a, is set by the evanescent decay length of the confining light, such that the mode spacing ($\approx \hbar^2/2Ma^2$) of the guide is comparable to one photon recoil energy. The cladding of the fiber protects the atoms from the environment, but it prevents access to the guided atom waves. In addition, spontaneous emission can limit atomic coherence.

Neutral particle waveguides based on current-carrying wires, originally suggested by Vladimirskiĭ for neutrons [16], have been extended to neutral atoms in the last five years [8–12]. Practical fabrication and heat dissipation issues limit the demonstrated characteristic size scale of these guides to > 100 μm, and the free-standing wire current densities to $< 10^5$ A/cm^2. Guiding of neutral atoms using a charged wire has also been proposed [13,14].

More recently, planar "slab" guides, which confine atoms along one dimension but leave two axes free or weakly confining, have been suggested [3,17,18] and demonstrated [19]. Some of these guides have much smaller transverse confinement scales (10–100 nm) than the above linear waveguides, and may be used to study weakly interacting two-dimensional systems [18]. Low-dimensionality traps are also viewed as a way to suppress photon reabsorption, an obstacle on the way to the realization of a continuous laser-like source of matter waves, the atom laser [3].

Waveguides that are tightly confining in *two* dimensions can similarly be used to form quasi-one-dimensional systems that do not have the impurities and high densities normally present in condensed matter systems. One of the interesting features of 1D systems is the possibility of "fermionization" of confined bosonic atoms [2,20]. Tightly confining potentials may also change the nature of atomic interactions from repulsive to attractive [2].

In this work we propose a tightly confining atomic waveguide based on the magnetic fields produced by patterns of planar microfabricated current-carrying wires. Since wires carrying a current I spaced a distance S apart produce magnetic field gradients that scale as I/S^2 and curvatures that scale as I/S^3, miniaturization of electromagnets can produce extremely high field gradients and curvatures [21]. We have previously demonstrated that "micro-electromagnets" (μEM) can be controlled dynamically with current densities of up to 10^8 A/cm^2 [22,23]. With standard electron-beam lithography, wire spacings < 100 nm can be achieved [24].

In the following sections, we describe the fields produced by several μEM waveguides (Sect. 2) and discuss confinement of atoms within these guides (Sect. 3). As with other atom guides, these guides can be used for incoherent transport without density loss due to free-flight expansion. However, we will focus on two exciting physical regimes accessible to μEM waveguides: the realization

[a] e-mail: joseph_thywissen@post.harvard.edu

[b] *Present address*: IGEN International Inc., 16020 Industrial Drive, Gaithersburg, MD 20877, USA.

of μK-deep single-mode waveguides (Sect. 3.1) and the use of tightly confining guides to study low-dimensional quantum degenerate gases of atoms (Sect. 3.2).

2 Parallel-wire waveguides for atoms

2.1 Principle of operation

A neutral atom with a permanent magnetic dipole moment $\boldsymbol{\mu}$ in a magnetic field $\mathbf{B}$ has a Zeeman potential $V = -\boldsymbol{\mu}\cdot\mathbf{B}$[1]. If $\boldsymbol{\mu}$ remains anti-aligned with $\mathbf{B}$ as it moves through the field, then $V = |\boldsymbol{\mu}|\,|\mathbf{B}| = \mu B$, and the atom can be confined near a field minimum. Fields that are confining in two (transverse) dimensions but not confining in a third (longitudinal) dimension are appropriate for use as linear waveguides for atoms. In this section, we discuss parallel-wire geometries that produce such guiding magnetic field configurations.

For example, four equally-spaced co-planar wires with anti-parallel currents can form a waveguide above the plane of the wires, as shown in cross-section in Figure 1a. Near its minimum, the guiding magnetic field is a two-dimensional quadrupole, whose characteristics will be discussed in detail in Sections 2.3 and 2.4. We will refer to the direction parallel to the wires as $\hat{z}$, the direction perpendicular to the substrate as $\hat{y}$, and the remaining orthogonal axis as $\hat{x}$.

Figure 1b shows an example of a fabricated four-wire waveguide guide. Each wire is 3 μm wide and 1 μm tall, and is able to carry 1.8 A, which is a current density $j \sim 10^8$ A/cm^2. Fabrication techniques for μEM's are described in reference [22]. Wires are formed on a substrate, which serves both to physically support the wires and to dissipate the heat produced. Furthermore, the resistance of the wires is reduced by cooling the substrate and wires to cryogenic temperatures. The cold substrate also acts as a cryopump, improving the vacuum conditions near the substrate.

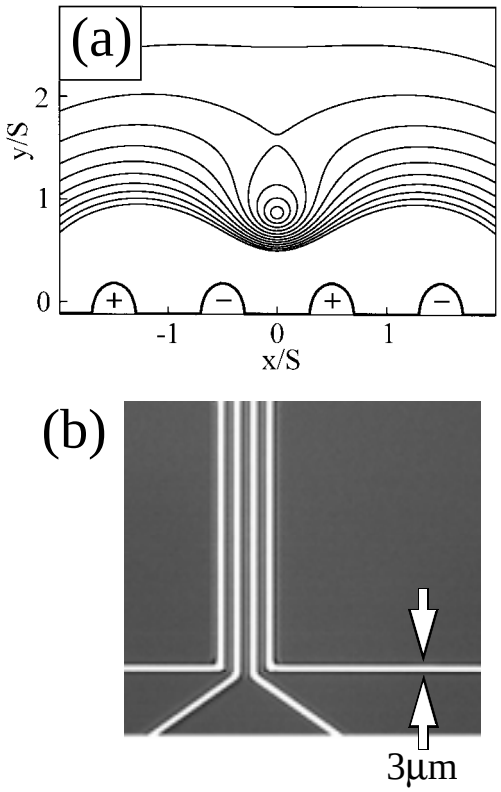

Fig. 1. (a) Isopotential curves for a four-wire microelectromagnet waveguide. Four wires, separated by a distance S and with anti-parallel current flow $\pm I$ (marked "+" and "−"), are mounted on a substrate. A potential minimum is formed above the wires and can be used to guide atoms in the out-of-plane direction $\hat{z}$. Twelve contours, equally spaced at $B_o/15$, are shown, where $B_o = \mu_o I/2\pi S$. (b) Micrograph of a fabricated four-wire guide. Wires are formed on a substrate, which serves both to support the wires mechanically and to dissipate the heat produced. Each wire is 3 μm wide and 1 μm high. We have demonstrated a continuous current capacity of 1.8 A for each wire, or approximately 10^8 A/cm^2.

2.2 Alternate waveguide configurations

Many parallel-wire configurations can create magnetic waveguides. Besides the four-wire guide shown in Figure 1a, several examples are: (a) a single wire with an external field B_e applied in the $\hat{x}$ direction (Fig. 2a); (b) a pair of wires with co-propagating currents (Fig. 2b); (c) a pair of wires with counter-propagating currents and an external field B_e in the $\hat{y}$ direction (Fig. 2c); and (d) three wires with each outer wire carrying more than half the current of the inner wire (Fig. 2d). A series of wires (not shown here), with or without external fields, can also form an array of guiding potentials [25]. In (a), the characteristic length scale S (analogous to the spacing in multi-wire guides) is the height of the minimum and determined by the external field: $S = \mu_o I/2\pi B_e$. Configuration (b) provides the highest field gradient for a given wire current I and spacing S, but also requires high-aspect-ratio wires because the zero occurs in the plane of the wire centers. Configurations (c) and (d) have a minimum whose position (in units of S) is adjustable.

In the following sections, we will focus on the four-wire waveguide configuration. This choice is somewhat arbitrary, but note that four-wire guides do not require external fields to form a minimum (as do (a) and (c)), high aspect ratios (as does (b)), or a nonzero net current (as do (a), (b), and (d)).

Similar magnetic fields could also be created at the micron length scale with magnetic recording technology [26]. Furthermore, 100-nm-scale patterning of magnetization in a material is possible, for instance, with scanning probe

[1] For strong enough fields, a quadratic Zeeman effect will become significant and can be used to confine neutral atoms that exhibit a hyperfine splitting [18]. Fields of this strength ($\approx$ 1 kG) will not be considered in the following sections, although they have been produced by μEM's [22].

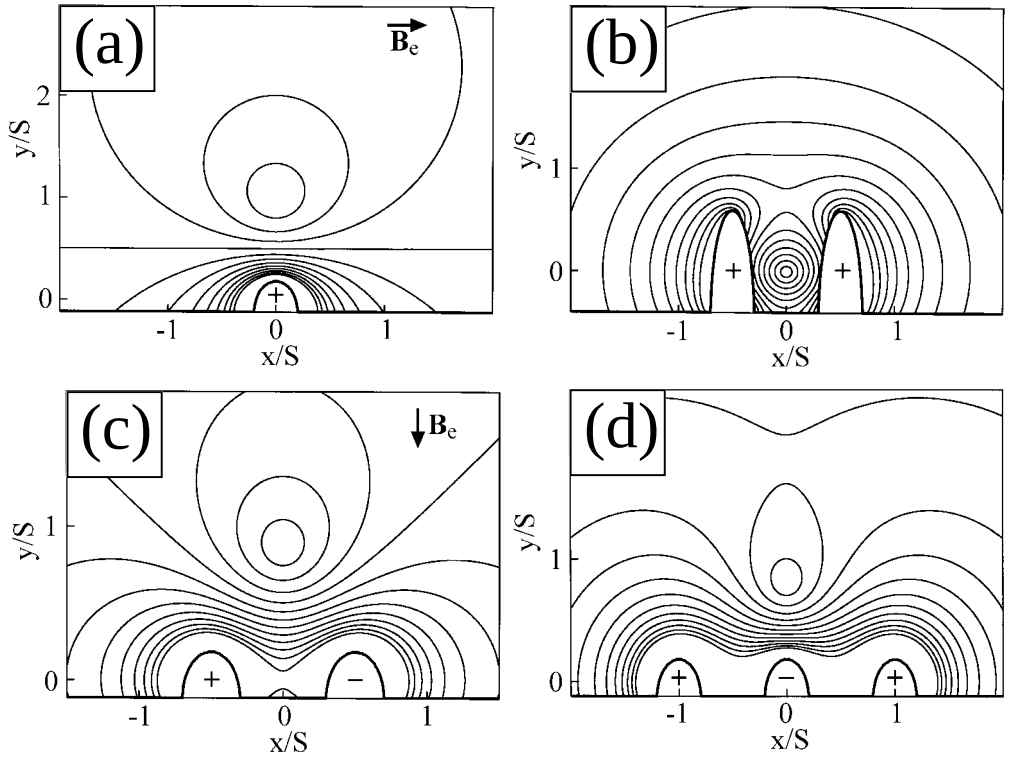

Fig. 2. Isopotential curves for several magnetic waveguide configurations. The direction of current flow is indicated by "+" and "−"; in-plane external magnetic fields are indicted by bold arrows. Twelve contours, equally spaced at $B_o/4$, are shown, where $B_o = \mu_o I/2\pi S$. (a) A single wire with an external field B_e applied in the $\hat{x}$ direction; here $S = \mu_o I/2\pi B_e$. (b) Two high-aspect-ratio wires, separated by S, with co-propagating currents. (c) Two wires, separated by S, with opposing current directions and an external field $B_e = B_o$ in the $\hat{y}$ direction. (d) Three wires, separated by S, with each outer wire carrying -1.25 times the inner-wire current.

or nanolithography techniques [27]. Permanent-magnet devices have the advantage that they do not need to be powered externally; however, with this advantage comes the inability to modulate the magnetic field dynamically. A further advantage of using small wires is experimental robustness: even if material purity, wire profile, or surface roughness changes along the length of the wires (or from one fabrication to the next), the potential is completely determined by the current – which is uniform along the length of the wire by Kirchoff's law – and by the wire spacing – which is well-defined lithographically.

2.3 Field characteristics

In this subsection, we analyze the location, depth, gradient, and curvature of the magnetic waveguide fields created by four co-planar cylindrical wires. A cylindrical wire has a field outside its surface that is indistinguishable from the field produced by an infinitesimally thin wire ("point wire"), according to Ampere's law. However, microfabricated wires will be flat at their contact with the substrate. By numerically integrating the Biot-Savart law, we find that wires with heights and widths smaller than half the inter-wire spacing S produce approximately the same gradient near the field minimum as do point wires. However, note that for finite wire heights, the plane of the wire centers ($y = 0$) does not coincide with the surface of the underlying substrate (see Figs. 1a and 2). These calculations also assume a uniform current distribution in the wires, which is valid for micron-scale gold wires carrying 10^8 A/cm^2 or less.

A four-wire waveguide with inner wires carrying opposing currents $\pm I$ and separated by S, and outer wires carrying opposing currents $\pm\beta I$ and separated by αS, will form a minimum above the plane of the wires when $1/\alpha < \beta < \alpha$ (see Fig. 1a). The minimum forms the center of the waveguide potential, and is located at $x = 0$ and $y = y_c$, where

$$y_c = \frac{S}{2}\sqrt{\frac{\alpha-\beta}{\beta-1/\alpha}}\,. \tag{1}$$

For $\alpha = 3$ and $\beta = 2$, $y_c = 0.39S$.

The depth of the four-wire guide is always limited by the maximum field in the $x = 0$ plane:

$$B_{\mathrm{depth}}/B_o = \begin{cases} 4(1-\beta/\alpha) & \text{if } \beta \geq \beta_D \\ 4\dfrac{(\sqrt{\alpha\beta}-1)^2}{(\alpha^2-1)} & \text{if } \beta < \beta_D \end{cases} \tag{2}$$

where $B_o = \mu_o I/2\pi S$ is the characteristic field above the guide, μ_o is the permeability of free space, and $\sqrt{\beta_D/\alpha} = \left(\alpha + \sqrt{2}(\alpha^2-1)\right)/(2\alpha^2-1)$. The depth is maximized at $\beta = \beta_D$, when the outer barrier ($y > y_c$) is equal to the inner barrier ($y = 0$). For example, at $\alpha = 3$ and $\beta = \beta_D = 2.13$, the waveguide depth is $1.16B_o$.

The radial gradient of the field magnitude near its conical minimum[2] is $B'_c = \kappa B_o/S$, where

$$\kappa = \frac{16}{(\alpha^2-1)^2\beta}\sqrt{(\alpha\beta-1)^5(1-\beta/\alpha)}. \quad (3)$$

The outer-wire current that maximizes the gradient is $\beta_\kappa = u(1+\sqrt{1+u^2/2})$, where $u = (3\alpha^2-1)/8\alpha$. For equally spaced wires, the gradient is maximized at $\beta_\kappa = 2.38$ to give $B'_c = 4.46\mu_o I/2\pi S^2$.

A weak axial ($\hat{z}$) field B_h must be applied[3] to maintain the adiabaticity of atoms moving near the center of the guide, as described in Section 2.4. This holding field creates a hyperboloid potential whose curvature at center is $(B'_c)^2/B_h$, where B'_c is the field gradient near center without B_h. The classical oscillation frequency of an atom with mass M near this quadratic minimum is

$$\omega_\perp = \sqrt{(\mu B'_c)^2/\mu M B_h}. \quad (4)$$

For the device shown in Figure 1b ($S = 5$ μm and $\alpha = 3$) with $I = 0.9$ A and $\beta = 2$, the field gradient the near guide center is $B'_c = 2.9\times10^6$ G/cm. In this guide, rubidium (^{87}Rb) confined in the $|F=2, m_F=+2\rangle$ state would have a classical oscillation frequency of $\omega_\perp = 2\pi\times1.1$ MHz and a level spacing of 52 μK, approximately five times the Rb magneto-optical trap (MOT) temperature of 10 μK [29]. The total guide depth would be 350 G, or 20 mK. Atomic hydrogen (H) in the $|F=1, m_F=+1\rangle$ state would have an oscillation frequency of $2\pi\times4.9$ MHz, a level spacing of 230 μK, and the same depth. These estimates assume $B_h = 12$ G, which ensures that the loss rate due to spin-flips near the field minimum is ~ 1 Hz, as described in the next section.

2.4 Loss rates

There are two loss mechanisms for a single atom within a four-wire magnetic guide: (1) spin flips near the magnetic field minimum, and (2) tunneling of the atom out of the confining potential. Depending on experimental conditions, collisions may also produce a significant loss rate, but we will not discuss collisional loss rates here. Surface-atom interactions may also be important, and are discussed in [30].

[2] Hexapole (*i.e.*, paraboloid) field minima can also be formed with micro-electromagnets. For example, a guide with $\alpha = \beta$ has a hexapole minimum between the inner two wires.

[3] Spin flips could also be avoided, as in [28], by modulating the current in the wires such that the field minimum rotates about the confined atoms at a frequency greater than $\omega_\perp$ but smaller than the Larmor procession frequency.

In order to remain in the low-field-seeking state, an atom must move through the field adiabatically. Near a quadratic minimum in field magnitude, this condition is met if the oscillation frequency ω is small compared to the Larmor procession frequency $\mu B_{min}/\hbar$, where B_{min} is the local field minimum.

For the four-wire waveguide discussed in Section 2.3, an external holding field $B_h\hat{z}$ adds in quadrature with the $\hat{x}\hat{y}$-fields produced by the wires to form a non-zero (Ioffe-type) minimum. The transverse oscillation frequency $\omega_\perp$ for an atom in this potential is given by (4). As B_h is increased, the rate of non-adiabatic spin flips is exponentially suppressed: Sukumar [31] gives the spin-flip loss rate of an atom in the ground state of this potential as

$$\Gamma_{SF}^{gnd} = C_{SF}\omega_\perp \exp\left[-\frac{\mu B_h}{\hbar\omega_\perp}\right], \quad (5)$$

where $C_{SF} = \pi/(2\sqrt{e}) \approx 0.95$ for a $J = 1/2$ atom. Since the spin flip loss rates of all other states are smaller than the ground state loss rate, we will use Γ_{SF}^{gnd} as a safe estimate of the lifetime of atoms in the guide. For $\mu B_h \gg \hbar\omega_\perp$, the loss rate of a $J = 1$ atom is lower than for the $J = 1/2$ atom since the exponential factor in (5) is multiplied by $4/\pi$ [31]; we will generally assume that (5) (with a $C_{SF} \sim 1$) gives a safe estimate of Γ_{SF}^{gnd} for atoms with $J \neq 1/2$.

Since an atom guided in a four-wire waveguide is not confined in a global minimum, we must consider tunneling loss rates out of the guide. In a one-dimensional potential $V(x)$, a bound state with an oscillation frequency ω_{osc} and energy E has the loss rate

$$\Gamma_T = C_T\omega_{osc}\exp\left[-2\int k(x)\mathrm{d}x\right], \quad (6)$$

where $k(x) = \sqrt{(2M/\hbar^2)(V(x)-E)}$, the integral limits are the classical turning points on either side of the potential, M is the mass of the particle, and C_T is a constant of order unity. The exponential component of (6) is the barrier transmission valid for small tunneling probabilities [32]. In contrast to Γ_{SF}, Γ_T is largest for the highest energy bound state, because $\int k(x)\mathrm{d}x$ is minimized. For our application, the particle is confined in a two-dimensional well; however, the loss rate is at most of order the one-dimensional loss rate across the path with the minimum value of $\int k(x)\mathrm{d}x$. We will assume C_T is of order unity and estimate tunneling rate for each state using this one-dimensional overestimate.

3 Applications

3.1 Coherent transport of atoms

When an experiment is sensitive to the phase accumulated by an atom wave during its transport through a waveguide, the existence of higher modes in the guide

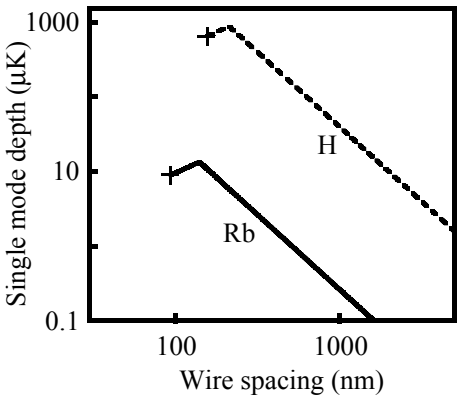

Fig. 3. The well depth (in μK) of single-mode atomic waveguides as a function of wire width (in nm), shown for both hydrogen (dashed line) and rubidium (solid line). The wire spacing shown is limited at + by the van der Waals interaction of the atom with the surface, as described in the text. For both cases shown, the optimal depth occurs at the cusp in the curve, which is the smallest spacing at which the depth is limited by the single-mode requirement (depth $\propto S^{-2}$) instead of the current density (depth $\propto S$).

is problematic. For instance, slight fluctuations in the coupling at the guide entrance can cause a time-dependent admixture of the first excited state that washes out fringes. This problem has been studied extensively for the case of fiber-based gyroscopes [33], for which applications researchers are careful to ensure higher modes are attenuated. However, conventional atom waveguides are single mode only at well depths of less than 100 nK [7]. In this section, we discuss how μEM waveguides can create a single mode guide deep enough to be loaded from a MOT. These depths are achieved by using sub-micron wire spacing, an application of nanolithography to atom optics.

To find the mode structure of atom waves propagating through a μEM waveguide, we solve numerically for the bound states in the two-dimensional transverse potential formed by a four-wire waveguide. Figure 3 shows the single-mode depth *versus* wire spacing for H with $\alpha = 3$ and $\beta = 2$ and for ^{87}Rb with $\alpha = 3$ and $\beta = 0.5$.

The wire spacing S determines the length scale of confinement for atom waves, and therefore for large S, single mode depth scales as S^{-2}. Assuming that wire width and height is proportional to S, the current density required to maintain this depth scales as S^{-3}. In Figure 3, we have constrained the current density to less than 10^8 A/cm^2, such that at low S, the possible depth scales as S; the maximum depth occurs at the transition from S to S^{-2} scaling. For H, at $S = 210$ nm and $I = 5.6$ mA, the depth is 0.9 mK and the oscillation frequency is $\omega_\perp = 2\pi \times 9.2$ MHz. For Rb, at $S = 140$ nm and $I = 2.5$ mA, the depth is 13 μK and $\omega_\perp = 2\pi \times 0.3$ MHz; this depth is comparable to the Rb MOT temperature. For both these examples, we choose a holding field such that $\Gamma_{\rm SF}^{\rm gnd} \sim 10^{-6}\omega_\perp$. The tunneling loss rates for H and Rb are $\Gamma_{\rm T} \sim 7 \times 10^{-7}\omega_\perp$ and $\Gamma_{\rm T} \sim 7 \times 10^{-8}\omega_\perp$, respectively.

At sub-micron length scales, strong attractive atom-surface forces put a lower bound on how close the guiding potential can be to the substrate. Using parameterizations of the van der Waals force that include its retardance at larger atom-surface separations [34], we restrict the spacings under consideration to those which produce a potential depth larger than the van der Waals shift at guide center[4]. This constraint sets a lower bound on S, marked by an "+" in Figure 3. Since the van der Waals force is stronger for Rb than for H [34], we chose the parameters $\alpha = 3$ and $\beta = 0.5$ (compared to $\beta = 2$ for H) to pull the center of the waveguide farther from the surface (see Eq. (1)).

One advantage of using co-planar wires to guide atoms is that the absence of physical confinement allows direct access to the confined atom wave. Two μEM guides can be brought into close enough proximity that an atom can tunnel from one guide to the next. A coherent atomic beamsplitter can be created: after an appropriate length, an atom wave that starts in one guide would exit with amplitude in both guides. This is the principle of operation for beamsplitters in fiber optical interferometers, and could be applied to atom wave interferometry as well.

3.2 Toward low-dimensional degenerate dilute atomic gases

In the multi-mode regime, the depth of the waveguide potential, and consequently the classical oscillation frequency in the center of the guide, are higher than in the single-mode case. The estimates presented above show that the values of the oscillation frequency in μEM waveguides can be two orders of magnitude higher than those in demonstrated atom guides: this allows a strong control of the strength of the inter-atomic interaction and opens rich opportunities for research on one-dimensional quantum degenerate atomic gases.

One of the most interesting features of one-dimensional (1D) systems is the existence, in many models, of a strict Boson-Fermion Duality (BFD): the possibility to express the same Hamiltonian in either bosonic or fermionic terms. The BFD is a direct consequence of *break-down of the spin-statistics connection in low-dimensions*. Several examples of BFD are known: the equivalence of the bosonic sin-Gordon model and fermionic massive Thirring model [35], the exact mapping between a gas of impenetrable bosons (a so-called "Tonks gas" [36]) and an ideal Fermi gas [20], and a recent generalization of the latter to the case of the δ-interacting bosons *versus* ϵ-interacting fermions mapping [37]. The μEM guides are an excellent tool for the creation of 1D impenetrable bosons and subsequent fermionization, because, as we will see below, the "impenetrability" regime requires low atomic densities and the upper bound for the density scales linearly

[4] Note that the constraint is conservative: the potential remains confining until the van der Waals force overwhelms the magnetic *gradient*, which occurs at smaller atom-surface separations.

with the frequency of the transverse confinement. Below, we give some estimates for the experimental parameters needed to realize such a project.

The effective 1D regime requires the temperature to be below the transverse energy spacing, $T \ll \hbar\omega_\perp$. As was shown recently [2], in this limit the two-body interaction potential between atoms at z_1 and z_2 is given by a 1D δ-potential

$$U(z_1, z_2) = g_{1\mathrm{D}}\delta(z_2 - z_1) \tag{7}$$

whose strength is

$$g_{1\mathrm{D}} = \frac{g_{3\mathrm{D}}}{2\pi b_\perp^2}\left(1 - \mathcal{C}\frac{a_{3\mathrm{D}}}{\sqrt{2}b_\perp}\right)^{-1}, \tag{8}$$

where $g_{3\mathrm{D}} = 4\pi\hbar^2 a_{3\mathrm{D}}/M$ is the interaction strength in free space, $a_{3\mathrm{D}}$ is the s-wave scattering length, $b_\perp = \sqrt{\hbar/M\omega_\perp}$ is the size of the transverse ground state, and $C = 1.4603\ldots$ [2].

Fermionization occurs when the 1D transmission coefficient associated with the interaction potential (7) becomes small: this happens in the low-energy scattering regime $k \ll 1/|a_{1\mathrm{D}}|$, where $\hbar k/M$ is a typical relative velocity and $a_{1\mathrm{D}} = 2\hbar^2/g_{1\mathrm{D}}M$ is the one-dimensional scattering length. For low temperatures, this typical wavevector of the relative motion is defined, in the case of a strong repulsive interaction, by the typical inter-atomic spacing $l \sim n_{1\mathrm{D}}^{-1}$ as $k \sim \pi/l$, where $n_{1\mathrm{D}}$ is the linear density. Therefore, at linear densities

$$n_{1\mathrm{D}} \ll 1/\pi\,|a_{1\mathrm{D}}| \tag{9}$$

the bosons become "impenetrable" and the system becomes thermodynamically indistinct from an ideal Fermi gas of the same density [20]. Since $1/\pi\,|a_{1\mathrm{D}}|$ is proportional to $\omega_\perp$ as long as $b_\perp \gg a_{3\mathrm{D}}$, *this regime is more easily observed at tighter confinements.*

In the opposite case, $n_{1\mathrm{D}} \gg 1/\pi\,|a_{1\mathrm{D}}|$, the system becomes a weakly interacting 1D Bose gas. For even higher densities $n_{1\mathrm{D}} \gtrsim \hbar\omega_\perp/g_{1\mathrm{D}}$ the mean field interactions induce a strong coupling to the higher transverse modes and the system becomes substantially three-dimensional.

Let us now estimate how high $\omega_\perp$ can be in a four-wire micro-electromagnet waveguide with demonstrated technologies. ^{87}Rb in the $|F = 2, m_\mathrm{F} = +2\rangle$ state in a guide with $S = 1$ μm, a current density $j = 1\times10^8$ A/cm^2, $\alpha = 4.9$, and $\beta = 3.7$ will have $\omega_\perp = 2\pi \times 3$ MHz and a ground state width $b_\perp = 6$ nm. These calculations assume a holding field $B_\mathrm{h} = 29$ G such that the lifetime in the guide $1/\Gamma_\mathrm{gnd} \approx 1$ second.

In Figure 4 we present the "phase diagram" (linear density $n_{1\mathrm{D}}$ *versus* temperature T) of a collection of ^{87}Rb atoms in a waveguide with a frequency $\omega_\perp = 2\pi\times0.3$ MHz. The "degenerate Fermi" domain corresponds to the strong fermionization, where the thermodynamic properties of the system will be equivalent to those of an ideal degenerate Fermi gas. We have not extended the Fermi/Bose border into the non-degenerate ("Boltzmann") regime ($n_{1\mathrm{D}} < 1/\lambda_{\mathrm{dB}}$), where quantum statistics are not evident in the thermodynamic properties of a gas.

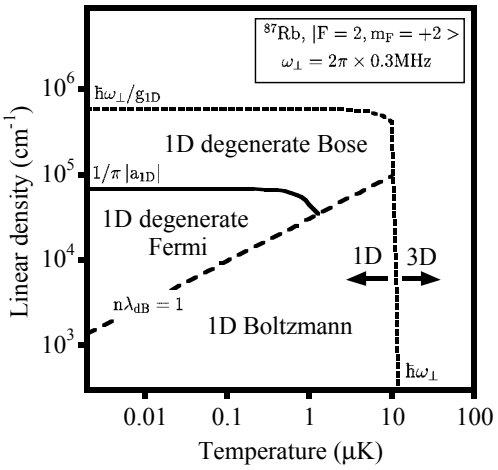

Fig. 4. Density-temperature "phase diagram" for a collection of ^{87}Rb atoms in a μEM waveguide, with $\omega_\perp = 2\pi \times 0.3$ MHz. Regions are delineated with three borders: (1) the transition from three-dimensional to one-dimensional dynamics occurs when the particle energy is comparable to transverse zero-point energy $\hbar\omega_\perp$; (2) the transition to impenetrability occurs when the typical 1D atom-atom transmission coefficient is 1/2; at low temperatures this occurs at $n_{1\mathrm{D}} = 1/\pi\,|a_{1\mathrm{D}}|$; (3) the border between degenerate and non-degenerate ("Boltzmann") gases is the line at which $n_{1\mathrm{D}}\lambda_{\mathrm{dB}}$ equals unity.

The $\omega_\perp$ chosen for Figure 4 requires a current density $j = 4 \times 10^6$ A/cm^2, only one twentieth of the capacity demonstrated by the device shown in Figure 1b. At tighter confinements, trap-induced modifications of scattering properties become important [2]. We observe that expression (8) predicts that a sign flip for the interaction strength $g_{1\mathrm{D}}$ will occur when $b_\perp = \mathcal{C}a_{3\mathrm{D}}/\sqrt{2}$. For ^{87}Rb, $a_{3\mathrm{D}} = +110a_{\mathrm{Bohr}}$ [38], and this signature of extremely tight confinement would require a current density of $j \sim 2 \times 10^8$ A/cm^2.

4 Conclusion

We have presented several planar wire configurations that form guiding potentials for atoms. Guiding atoms with magnetic fields produced by microfabricated or nanofabricated electromagnets avoids the size scale and spontaneous emission constraints imposed by using quasi-resonant light. In the high transverse field gradients (10^7 G/cm) and curvatures (10^{12} G/cm^2) produced by μEM's, guided ^{87}Rb atoms can have transverse mode energy spacings greater than 50 μK. Fields created with electromagnets can also be controlled dynamically and are robust against changes in material properties.

Atomic funnels are a natural extension of the parallel-wire geometries analyzed in this work. Since the radius of the confining potential is proportional to the wire spacing S, if S is large at the entrance of a waveguide and becomes smaller along its length, the guide can act as a funnel. A funnel can facilitate loading into small diameter guides,

or (in reverse) can adiabatically compress the transverse atomic momenta at the exit of a waveguide.

We have shown that μEM waveguides can operate in a single-mode regime with depths comparable to temperatures of a MOT. Two μEM guides can be brought into close enough proximity that an atom can tunnel from one guide to the next, creating a waveguide-based atomic beamsplitter. The nearly arbitrary planar geometries possible with conventional lithography techniques suggest that many elements such as waveguides and beamsplitters might be fabricated on a single substrate to create "integrated" atom optics.

Finally, we have shown that atoms are sufficiently tightly confined in a μEM guide to permit (a) the trap-induced transformation of 1D scattering properties from repulsive ($a_{1D} > 0$) into attractive ($a_{1D} < 0$), or (b) the fermionization of a strongly interacting bosonic ensemble. The latter effect is a clear demonstration of the breakdown of the spin-statistics connection in low dimensions.

The authors thank N. Dekker, C. Lee, A. Barnett for useful discussions. This work was supported by National Science Foundation Grant Numbers: PHY-9312572, PHY-9732449, and DMR-9809363.

References

1. W. Ketterle, N.J. van Druten, Phys. Rev. A **54**, 656 (1996).
2. M. Olshanii, Phys. Rev. Lett. **81**, 938 (1998).
3. M. Olshanii, Y. Castin, J. Dalibard, in *Proceedings of the XII Conference on Laser Spectroscopy*, edited by M. Inguscio, M. Allegrini, A. Sasso (World Scientific 1995); T. Pfau, J. Mlynek, OSA Trends Opt. Photon. **7**, 33 (1997); Y. Castin, J.I. Cirac, M. Lewenstein, Phys. Rev. Lett. **80**, 5305 (1998).
4. H. Monien, M. Linn, N. Elstner, Phys. Rev. A **58**, R3395 (1998).
5. M.A. Ol'Shanii, Yu.B. Ovchinnikov, V.S. Lethokhov, Opt. Commun. **98**, 77 (1993); S. Marksteiner, C.M. Savage, P. Zoller, S.L. Rolston, Phys. Rev. A **50**, 2680 (1994).
6. M.J. Renn, D. Montgomery, O. Vdovin, D.Z. Anderson, C.E. Wieman, E.A. Cornell, Phys. Rev. Lett. **75**, 3253 (1995); M.J. Renn, E.A. Donley, E.A. Cornell, C.E. Wieman, D.Z. Anderson, Phys. Rev. A **53** R648 (1996); H. Ito, T. Nakata, K. Sakaki, M. Ohtsu, K.I. Lee, W. Jhe, Phys. Rev. Lett. **76**, 4500 (1996).
7. For reviews of light-based atom waveguides, see: J.P. Dowling, J. Gea-Banacloche, Adv. At. Mol. Opt. Phys. **37**, 1 (1996); V.I. Balykin, Adv. At. Mol. Opt. Phys. **4**, 181 (1998).
8. J. Schmiedmayer, Phys. Rev. A **52**, R13 (1995); J. Schmiedmayer, Appl. Phys. B **60**, 169 (1995); L.V. Hau, J.A. Golovchenko, M.M. Burns, Phys. Rev. Lett. **74**, 3138 (1995).
9. C.J. Myatt, N.R. Newbury, R.W. Ghrist, S. Loutzenhiser, C.E. Wieman, Opt. Lett. **21**, 290 (1996).
10. J.A. Richmond, S. Nic Chormaic, B.P. Cantwell, G.I. Opat, Acta Phys. Slov. **48**, 481 (1998).
11. J. Fortagh, A. Grossman, C. Zimmerman, T.W. Hänsch, Phys. Rev. Lett. **81**, 5310 (1998).
12. J. Denschlag, D. Cassettari, J. Schmiedmayer, Phys. Rev. Lett. **82**, 2014 (1999).
13. L.V. Hau, M.M. Burns, J.A. Golovchenko, Phys. Rev. A **45**, 6468 (1992).
14. J. Schmiedmayer, Eur. Phys. J. D **4**, 57 (1998).
15. H. Ito, K. Sakaki, M. Ohtsu, W. Jhe, App. Phys. Lett. **70**, 2496 (1997).
16. V.V. Vladimirskiĭ, Sov. Phys. JETP **12**, 740 (1961).
17. Yu.B. Ovchinnikov, S.V. Shul'ga, V.I. Balykin, J. Phys. B **24**, 3173 (1991); P. Desbiolles, J. Dalibard, Opt. Commun. **132**, 540 (1996); W.L. Power, T. Pfau, M. Wilkens, Opt. Commun. **143**, 125 (1997).
18. E.A. Hinds, M.G. Boshier, I.G. Hughes, Phys. Rev. Lett. **80**, 645 (1998).
19. H. Gauck, M. Hartl, D. Schneble, H. Schnitzler, T. Pfau, J. Mlynek, Phys. Rev. Lett. **81**, 5298 (1998).
20. D.B. Creamer, H.B. Thacker, D. Wilkinson, Phys. Rev. D **21**, 1523 (1980); V.E. Korepin, N.M. Bogoliubov, A.G. Izergin, *Quantum Inverse Scattering Method and Correlation Functions* (Cambridge University Press, Cambridge, 1993), Appendix I.1.
21. J.D. Weinstein, K.G. Libbrecht, Phys. Rev. A **52**, 4004 (1995).
22. M. Drndić, K.S. Johnson, J.H. Thywissen, M. Prentiss, R.M. Westervelt, App. Phys. Lett. **72**, 2906 (1998).
23. K.S. Johnson, M. Drndić, J.H. Thywissen, G. Zabow, R.M. Westervelt, M. Prentiss, Phys. Rev. Lett. **81**, 1137 (1998).
24. Wires with widths as small as 10 nm have been formed with electron beams on polymeric resists: see H.G. Craighead, in *Physics of Nanostructures*, edited by J.H. Davies, A.R. Long (Institute of Physics Publishing, Bristol, 1992), p. 25.
25. G. Zabow, M. Drndić, J.H. Thywissen, K. Johnson, R.M. Westervelt, M. Prentiss, Eur. Phys. J. D **7**, 351 (1999).
26. E.A. Hinds, in *New Directions in Atomic Physics*, edited by C.T. Whelan (Plenum, in press).
27. S. Manalis, K. Babcock, J. Massie, V. Elings, M. Dugas, App. Phys. Lett. **66**, 2585 (1995); R.L. White, R.M.H. New, R.F.W. Pease, IEEE Trans. Mag. **33**, 990 (1997).
28. W. Petrich, M.H. Anderson, J.R. Ensher, E.A. Cornell, Phys. Rev. Lett. **74**, 3352 (1995).
29. C.D. Wallace, T.P. Dinneen, K.Y.N. Tan, A. Kumarakrishnan, P.L. Gould, J. Javanainen, J. Opt. Soc. Am B **11**, 703 (1994).
30. C. Henkel, M. Wilkens, `quant-ph/9902009`.
31. C.V. Sukumar, D.M. Brink, Phys. Rev. A **56**, 2451 (1997).
32. E. Merzbacher, *Quantum Mechanics*, 2nd edn. (John Wiley & Sons, New York, 1970), p. 126.
33. S. Ezekiel, in *Fiber-Optic Rotation Sensors and Related Technologies*, edited by S. Ezekiel, H.J. Arditty (Springer-Verlag Berlin 1982), p. 25.
34. G. Vidali, G. Ihm, H.-Y. Kim, M.W. Cole, Surf. Sci. Rep **12**, 133 (1991); A. Shih, V.A. Parsegian, Phys. Rev. A **12**, 835 (1975); C. Carraro, M.W. Cole, Prog. Surf. Sci. **53**, 61 (1998).
35. S. Coleman, Phys. Rev. D **11**, 2088 (1975).
36. L. Tonks, Phys. Rev. **50**, 955 (1936); M. Girardeau, J. Math. Phys. **1**, 516 (1960); A. Lenard, J. Math. Phys. **7**, 1268 (1966).
37. T. Cheon, T. Shigehara, Phys. Rev. Lett. **82**, 2536 (1999).
38. J.R. Gardner, R.A. Cline, J.D. Miller, D.J. Heinzen, H.M.J.M. Boesten, B.J. Verhaar, Phys. Rev. Lett. **74**, 3764 (1995).